BIOLOGIA PLANTARUM 59 (3): 570-580, 2015 DOI: 10.1007/s10535-015-0519-9

NADPH oxidase RBOHD contributes to autophagy and hypersensitive cell death during the plant defense response in *Arabidopsis thaliana*

H.B. LIU[1,2,3], X.D. WANG[1], Y.Y. ZHANG[3], J.J. DONG[1,2], C. MA[1,2], and W.L. CHEN[1]*

MOE Key Laboratory of Laser Life Science and Institute of Laser Life Science, College of Biophotonics, South China Normal University, Guangzhou 510631, P.R. China[1]
Guangdong Key Laboratory of Biotechnology for Plant Development, College of Life Science, South China Normal University, Guangzhou 510631, P.R. China[2]
Department of Plant Biology and Ecology, College of Life Sciences, Nankai University, Tianjin 300071, P.R. China[3]

Abstract

Autophagy has been implicated as a cellular protein degradation process that is used to recycle cytoplasmic components under biotic and abiotic stresses and so restrict programmed cell death (PCD). In this study, we report a novel regulatory mechanism by which NADPH oxidase respiratory burst oxidase homolog D (RBOHD) regulated pathogen-induced autophagy and hypersensitive (HR) cell death. We found that the *Pseudomonas syringae* pv *tomato* bacteria DC3000 expressing *avrRps4* (*Pst-avrRps4*) induction of RBOHD-dependent reactive oxygen species (ROS) production promoted the onset of autophagy, whereas a pretreatment with an NADPH oxidase RBOHD inhibitor reversed this trend. The inhibitor significantly blocked pathogen-induced autophagosome formation and ROS increase. Moreover, we also show that in the wild-type and *atrbohF* mutant, *Pst-avrRps4*-induced cell death was limited, whereas in the case of the *atrbohD* mutant, the infection triggered a spreading-type necrosis. Our results demonstrate that the RBOHD-dependent ROS accumulation stimulated autophagosome formation and limited HR cell death.

Additional key words: mutants, pathogen resistance, programmed cell death, *Pst-avrRps4*.

Introduction

Plants have evolved multiple defense responses against pathogen attacks. A typical response is rapid cell death in plant leaves at the infection site, which is known as the hypersensitive response programmed cell death (HR PCD) (Liu *et al*. 2005). The HR PCD is triggered upon infection by an avirulent pathogen to limit both the spread of cell death and the pathogen, and it protects healthy adjacent cells from pathogen attack (Lam 2004, Seay *et al*. 2009). Autophagy is induced in the plant defense response against pathogens, and it leads to a negative regulation of PCD (Liu *et al*. 2005, Seay *et al*. 2006). In *Arabidopsis* plants, both the formation of autophagosomes and the expression of some *autophagy-related* (*ATG*) genes are induced during nutrient starvation and pathogen infection, including *ATG2*, *ATG7*, and *ATG8a* (Doelling *et al*. 2002, Slavíková *et al*. 2005, Lai *et al*. 2011, Wang *et al*. 2011). These *Arabidopsis ATG* genes are involved in a constitutive autophagy in plant root tip cells (Doelling *et al*. 2002, Slavíková *et al*. 2005, Inoue *et al*. 2006, Wang *et al*. 2011).

The NADPH oxidase is the major source of signaling reactive oxygen species (ROS) under various abiotic and biotic stresses (Wojtaszek 1997, Bolwell *et al*. 1998, Jiang and Zhang 2002, Liu *et al*. 2012) and the autophagy can be induced by ROS (Xiong *et al*. 2007). The NADPH oxidase inhibitor diphenylene iodinium (DPI) blocks autophagy induction upon nutrient starvation and salt stress, but not during osmotic stress (Liu *et al*. 2009). DPI also does not inhibit the constitutive autophagy in RNAi-*AtTOR* lines indicating that *AtTOR* acts either

Submitted 15 July 2014, *last revision* 2 January 2015, *accepted* 8 January 2015.
Abbreviations: *ATG* - autophagy-related genes; BTH - benzothiadiazole; DAB - 3,3′-diaminobenzidine; DCF - 2′,7′-dichlorofluorescein diacetate; DPI - diphenylene iodinium; HR - hypersensitive response; PCD - programmed cell death; *PR* genes - pathogen-related genes; RBOHD - respiratory burst oxidase homolog D; RPS4 - resistance to *Pseudomonas syringae* 4; SA - salicylic acid; WT - wild type.
Acknowledgments: This study was supported by the National Natural Science Foundation of China (31170250) and Natural science Foundation of Guangdong Province (2014A030313420). We are grateful to Richard D. Vierstra (the Department of Genetics, the University of Wisconsin, Madison, USA) for kindly providing the *Arabidopsis thaliana* seeds stably expressing 35S:GFP-ATG8a.
* Corresponding author; fax: (+86) 20 8521 6052, e-mail: chenwl@scnu.edu.cn

downstream of NADPH oxidase or that it works in a parallel pathway to NADPH oxidase (Liu and Bassham 2010). *Arabidopsis* homologs of the mammalian gp91^{phox} respiratory burst membrane-bound NADPH oxidase subunit are encoded by a 10-member gene family from *AtrbohA* to *AtrbohJ* (Torres and Dangl 2005). The *AtrbohD* and *AtrbohF* are the most highly expressed *Atrboh* genes, whereas other *Rboh* genes are maintained at very low levels of expression (Torres *et al*. 2002).

Several studies showed that autophagy is essential for limiting the spread of cell death during the plant defense response (Liu *et al*. 2005, Patel and Dinesh-Kumar 2008, Yoshimoto *et al*. 2009). Autophagy-deficient mutants, when compared to wild type (WT), show no obvious phenotypic differences during most of their life cycles. However, enhanced leaf senescence is observed when grown in carbon- and nitrogen-deprived conditions (Hanaoka *et al*. 2002, Xiong *et al*. 2005), and the spread of cell death enhances in autophagy-deficient mutants after infection (Liu *et al*. 2005, Patel and Dinesh-Kumar 2008). Yoshimoto *et al*. (2009) found that an older autophagy-deficient mutant *atg5* shows the spread of cell death, but this is not observed in WT after infection with *Pst-avrRpm1*. Additionally, a low contant of salicylic acid (SA) in young plants is maintained, whereas mature plants have a higher content of SA after pathogen infection (Yoshimoto *et al*. 2009). Similarly, *atrbohD* mutants hyperaccumulate SA and exhibit an increased spread of cell death compared with WT after inoculation with *Alternaria brassicicola* strain CBS 125088 (Pogány *et al*. 2009). This indicates that SA or RBOHD may play an important role in regulating cell death. The SA positively regulates cell death interplay with RBOHD, and autophagy negatively regulates pathogen induced cell death by SA signaling. However, a relationship among RBOHD, autophagy, and cell death is not clear.

The aim of the paper was to elucidate molecular mechanisms associated with autophagy, RBOHD, and HR PCD in *Arabidopsis* during the plant innate immune response.

Materials and methods

AtrbohD-3 (NASC code N9555), *atrbohF-3* (NASC code N9557), and *atrbohD/F* (NASC code N9558) mutants of *Arabidopsis thaliana* L. (WT, ecotype Columbia) were obtained from the European *Arabidopsis* Stock Centre (NASC). *AtrbohD* × *GFP-ATG8a* plants were generated by crossing *atrbohD* mutants with GFP-ATG8a plants. The plants were grown in Murashige and Skoog (MS) medium or in pots with soil in growth chambers at a temperature of 22 °C, a relative humidity of 82 %, a 16-h photoperiod, and an irradiance of 120 μmol m^{-2} s^{-1}. For plate-grown plants, seeds were surface sterilized and sown on a solid MS medium.

Infections with virulent or avirulent *Pst* DC3000 strains were performed as previously described (Hofius *et al*. 2009). For pathogen-induced spreading HR cell death, bacteria were hand-infiltrated *via* a needleless syringe with 2.5×10^7 CFU cm^{-3}, and bacterial growth in plant leaves was measured as previously described (Patel and Dinesh-Kumar 2008). To obtain the bacterial count, six-week-old *Arabidopsis* leaves were infiltrated with 1×10^6 CFU cm^{-3} bacterial suspension, the leaves were harvested at 0, 2, and 4 d post-infection with pathogens (dpi), leaf discs were surface sterilized using 70 % (v/v) ethanol for 1 min, and dilutions to 10^{-2}, 10^{-3}, and 10^{-4} were performed.

One-week-old *Arabidopsis* seedlings were inoculated with a 1×10^7 CFU cm^{-3} bacterial suspension in 10 mM $MgCl_2$ for 3 h, and subsequently washed with sterile water. The seedlings were immediately vacuum infiltrated with 1 μM *LysoTracker Red* (*LTR*, *Molecular Probes*, Eugene, OR, USA) and kept in the dark for an additional hour before visualization with a *Zeiss LSM 510* laser scanning microscope (LCSM, *LSM510/ConfoCor2*, *Carl-Zeiss*, Jena, Germany) using a 543 nm excitation and a *BP565-625* nm emission filters. GFP-AtATG8a transgenic seedlings were visualized by confocal microscopy using a 488 nm excitation and a *BP505-550* nm emission filters. Confocal images were visualized with the *Zeiss LSM 510* with 40× and 100× oil-immersion objectives, and analyzed using the *Zeiss Rel 3.2* image processing software. For inhibitor studies, seedlings were inoculated with *Pseudomonas syringae* pv. *tomato* bacteria DC3000 (*Pst-avrRps4*) suspensions for 1 h and then transferred to 10 mM $MgCl_2$ with or without 20 μM DPI for 3 h. The DPI dissolved in dimethyl sulfoxide (DMSO) and an equivalent volume of pure DMSO were added as controls, and autophagosome structures were quantified using methods that were previously described (Liu *et al*. 2009).

Protoplast isolation from *Arabidopsis* plants (6-week-old) was performed according to a modified procedure (Mackey *et al*. 2003, Bi *et al*. 2009). Briefly, well-expanded leaves were sliced into strips (0.5 - 1 mm) with a razor blade, and vacuum-infiltrated with an enzyme solution (0.4 %, m/v) macerozyme R10 (*Yakult Honsha*, Tokyo, Japan), 1.5 % (m/v) cellulase R10 (*Yakult Honsha*), 20 mM MES buffer; pH 5.7, 0.4 mM mannitol, 10 mM $CaCl_2$, and 20 mM KCl for 15 - 20 min. The digestion was continued in the dark without shaking for 3 h at room temperature. The enzyme/protoplast solution was filtered through a 75-μM pore nylon mesh, and then centrifuged at 100 *g* and 25 °C for 3 min to pellet protoplasts in a round-bottomed tube. The protoplast pellet was resuspended using a W5 solution containing 125 mM $CaCl_2$, 154 mM glucose, 5 mM KCl, and 1.5 mM MES/potassium acetate (pH 5.6).

Cellular and extracellular ROS accumulation was visualized using 3,3′-diaminobenzidine (DAB) and 2′,7′-dichlorofluorescein diacetate (DCF) staining as previously described (Pogány *et al*. 2009). For DAB

staining, leaves were collected 24 h after inoculation with the bacteria at 2.5×10^7 CFU cm^{-3}. For DCF staining, protoplasts were inoculated with 1×10^7 CFU cm^{-3} avirulent bacteria for 0.5 h, and then washed with a W5 solution. The protoplasts were incubated with DCF at a final concentration of 5 mM, and the production of ROS was visualized under the *Zeiss LSM510* laser scanning microscope using an excitation at 488 nm and the *BP505-550* nm emission filter. Chlorophyll-derived red fluorescence (488 nm excitation) was visualized at 650 nm with a long-pass filter (Gao *et al*. 2013). The fluorescence of DCF was determined using an *LS55* luminescence spectrophotometer (*Perkin Elmer*, Bucks, UK) as previously described (Mackey *et al*. 2003). For inhibitor studies, protoplasts were inoculated with 1×10^7 CFU·cm^{-3} avirulent bacteria + 20 μM DPI for 0.5 h.

Detection of cell death by lactophenol-trypan blue staining was performed as previously described (Pogány *et al*. 2009). The number of dead cells was statistically analyzed using methods described in Hofius *et al*. (2009). Leaves were collected 24 h after inoculation with bacteria at 2.5×10^7 CFU·cm^{-3}.

Leaves of 6-week-old plants were inoculated with 1×10^8 CFU cm^{-3} bacteria, and total RNA was extracted using *TRIzol* reagent (*Invitrogen*, Guangzhou, China). For reverse transcription, cDNA was generated from 1 μg of total RNA using reverse transcriptase *M-MLV* (*TaKaRa*, Dalian, China). Primers used for RT-PCR are shown in Table 1.

Experimental data are expressed as means ± SE or SD. Statistical data were analyzed using *ANOVA* and the Student's *t*-test ($\alpha = 0.05$).

Table 1. The list of gene-specific primers.

Gene	Forward primer sequence (5'-3')	Reverse primer sequence (5'-3')	Acc. No.	Length [bp]	Tm [°C]	Number of cycles
ATG2	ATGGTGTTTCCGTGGCATT	AGGATAGTGTAGCTGGAGGCGT	AT3G19190	1090	55	30
ATG7	GACGAAGGTTTCTGGCATAG	TCATTACAAGCAGCGGATAC	AT5G45900	512	55	30
ATG8a	ATGATCTTTGCTTGCTTGA	AGCAACGGTAAGAGATCCA	AT4G21980	414	52	28
PR1	CTCAAGATAGCCCACAAGATT	GCGTAGTTGTAGTTAGCCTTCT	AT2G14610	250	52	28
PR2	ATGTCTGAATCAAGGAGCTTAGC CTCACCACC	GTTGAAATTAACTTCATACTTAGA CTGTCGATCTGG	AT3G57260	1020	58	28
RPS4	TTCGGCTGAAGCAATGAG	GTCGCGGTCTAAGCTCGT	AT5G45250	286	55	30
RBOHD	ATGAAAATGAGACGAGGCAATTC	GATGCGTGAGGAGGTGCTT	AT5G47910	408	55	30
ACTIN	ATGGTGAAGGCTGGATTTGC	CATCACCAGAATCCAGCACAA		427	55	28

Results

To investigate the process of autophagy in plants, we used WT and *atrboh* mutant *Arabidopsis* plant seedlings that were challenged with virulent or avirulent pathogens. Autophagosomes formation was followed by confocal microscopy after staining the seedlings with the autophagosome-specific dye *LTR* (Liu *et al*. 2005). The control seedlings and those inoculated with avirulent *Pst* DC3000 did not accumulate autophagosomes (Fig. 1*A*,*B*); this indicates that neither *Pst* DC3000 nor $MgCl_2$ induced autophagy. In contrast, we found that the *Pst-avrRps4*-infected cells analyzed at 3 h post infection (hpi) accumulated abundant autolysosomal-like structures in WT indicating that autophagy can be activated by this avirulent bacterium (Fig. 1*C*).

When the mutant line *atrbohF* was infected with *Pst-avrRps4*, the formation of numerous autophagosomes was observed. In contrast, in the case of *atrbohD* and *atrbohD/F* double mutant, autophagosomes were rarely observed (Fig. 1*D*,*E*,*F*). The number of LTR-stained autophagosomes per root section was also analyzed (Fig. 1*G*). Compared to the control conditions and *atrbohD* mutant, significantly more autophagosomes were detected upon *Pst-avrRps4* inoculation in the WT and *atrbohF* plants. These data indicate that RBOHD was possibly required for autophagy that was induced by avirulent *Pst-avrRps4*. To determine if autophagy was induced by an avirulent pathogen, we also monitored autophagy activity in seedlings that stably expressed GFP-ATG8a. Autophagosomes were detected by confocal microscopy *via* direct visualization of the GFP-ATG8a marker (Fig. 2) (Thompson *et al*. 2005). Compared to *Pst* DC3000 and the control conditions, significantly more autophagosomes were detected after the *Pst-avrRps4* inoculation (Fig. 2*A*,*B*,*C*). The results are consistent with LTR labeling autophagosomes in WT (Fig. 1*A*,*B*,*C*), which indicates that *Pst-avrRps4* could induce autophagy.

The burst of extracellular ROS mainly originates from plasma membrane-bound NADPH oxidase RBOHD, and DPI can efficiently inhibit the activity of RBOHD when *Arabidopsis* plants are under stress (Torres *et al*. 2002, Ogasawara *et al*. 2008, Yun and Chen 2011). To study the potential role of RBOHD and ROS in autophagy, we monitored autophagy activity *via* the green fluorescent protein (GFP) label in the GFP-ATG8a transgenic plants in combination with the DPI treatment (Fig. 2). Autophagosomes were rarely observed under the control conditions, which indicates that neither DPI nor DMSO

induced autophagy (Fig. 2*G*,*H*). After the inoculation with *Pst-avrRps4*, numerous autophagosomes were observed in the absence of DPI (Fig. 2*F*), but no autophagosomes were observed after adding DPI (Fig. 2*E*). Autophagosomes were also rarely seen in the *atrbohD* × *GFP-ATG8a* plants (Fig. 2*D*). To quantify the effects of DPI or RBOHD on autophagosome formation, we analyzed the number of autophagosomes per root section (Fig. 2*I*). This confirmed that after the *Pst-avrRps4* infection, the number of autophagosomes dramatically decreased in the *atrbohD* × *GFP-ATG8a* plants or after incubation with DPI. We then analyzed the expression of *RBOHD* in roots of seedlings after the infection with avirulent *Pst-avrRps4*. As expected, *RBOHD* expression levels increased after the pathogen induction (Fig. 1 Suppl.). These results suggest that autophagy was regulated by an RBOHD-dependent pathway during the *Pst-avrRps4* infection, which might involve ROS as signal.

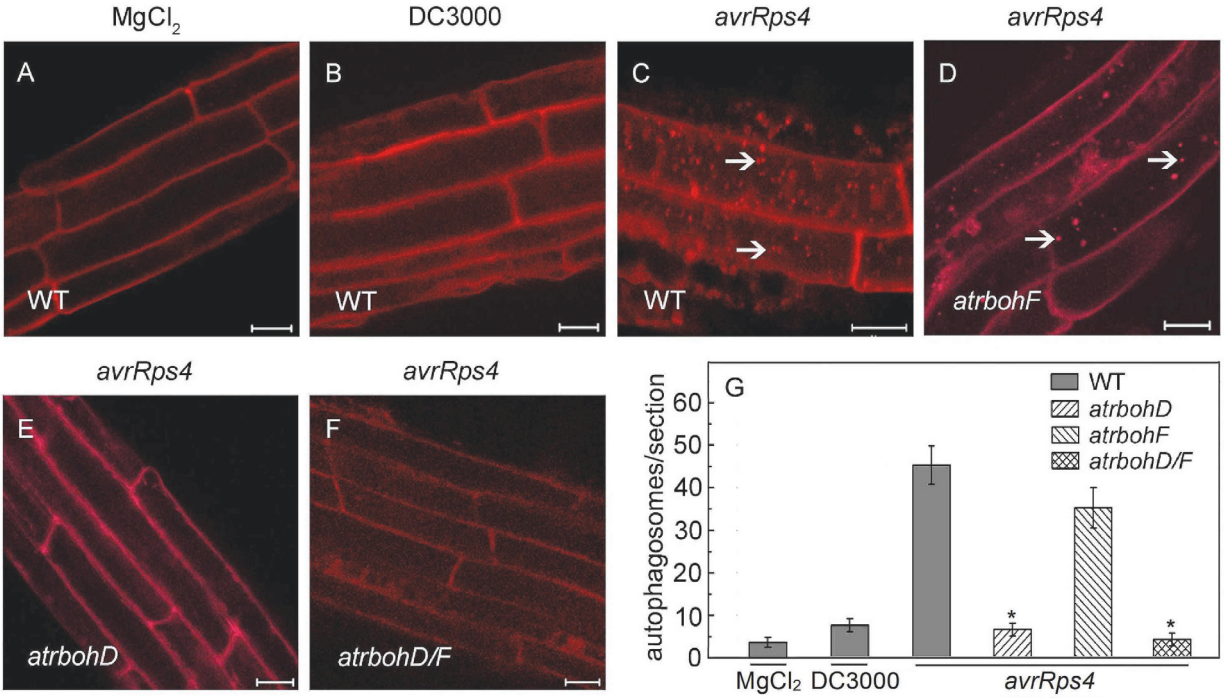

Fig. 1. Autophagy is induced by an avirulent pathogen infection. One-week-old WT seedlings (*A* - *C*) were inoculated with $MgCl_2$ or *Pst* DC3000 or *Pst-avrRps4* for 3 h followed by LTR staining. One-week-old *atrbohF* (*D*), *atrbohD* (*E*) and *atrbohD/F* (*F*) mutant seedlings were inoculated with avirulent *Pst-avrRps4* for 3 h followed by LTR staining. *Bars* = 20 μm. The number of LTR-stained autophagosome-related structures per root section was counted 3 h after inoculation (*G*). Means and SE were calculated from three seedlings per treatment. Results were reproduced in three independent experiments. *Asterisks* indicate a significant difference from WT treated with *avrRps4* ($P < 0.05$; Student's *t* test).

In addition to the macroscopic evaluation of *Pst-avrRps4*-induced disease symptoms, microscopic studies were performed on the *atrboh* mutants to observe extracellular ROS and cell death responses that were dependent on functional RBOHD. The ROS were detected by DAB and DCF, and cell death was detected by trypan blue staining (Fig. 4). We show that after the *Pst-avrRps4* inoculation, ROS accumulated in the WT and *atrbohF* mutants, whereas no ROS production was found 24 hpi in the *atrbohD* mutant (Fig. 4*A*). This indicates that RBOHD was required for ROS production in the plant defense response. To visualize the location and production of ROS in cells during the process of pathogen invasion, protoplasts were inoculated with *Pst-avrRps4*. We found that DCF fluorescence increased after 1 h, and ROS were mainly located in the plasma membrane (Fig. 5*A*,*C*). In contrast, no detectable DCF signal was found in protoplasts pretreated with DPI or $MgCl_2$ (Fig. 5*A*,*C*). In protoplasts of the *atrbohD* mutant, no increase in DCF signal was found (Fig. 5*B*,*C*). These data demonstrate that ROS mainly originated from plasma membrane-bound NADPH oxidase RBOHD during the early immune response. Further, we investigated whether the spread of cell death was also exhibited in the *atrboh* mutants. We found that in the WT and *atrbohF* mutant plants infected with *Pst-avrRps4*, cell death was confined to the pathogen infection site after 4 dpi, and it did not expand at 8 dpi (Fig. 3). However, in the *atrbohD* plants, cell death extended beyond the site of pathogen infection into healthy, uninfected tissue (Fig. 3). At 8 dpi, the cell death in the *atrbohD* plants expanded to the most of leaf, which resulted in the death of the infected leaf (Fig. 3). This phenotype was especially prominent in older leaves of the 6-week-old plants as

compared to young leaves of the three- or four-week-old plants. In contrast, the infection with *Pst* DC3000 resulted in unlimited cell death in the WT and *atrboh* mutants (Fig. 3). These results suggest that RBOHD was also required to limit *Pst-avrRps4*-induced cell death to the infection site.

Using the trypan-blue staining assay, we monitored cell death areas after mock ($MgCl_2$) and *Pst-avrRps4* inoculation. There were no differences between the WT and *atrboh* mutants after the mock treatment, in all of them cell death was rarely observed. However, after the *Pst-avrRps4* infection, cell death occurred, and both WT and *atrbohF* displayed less trypan blue staining than *atrbohD* (Fig. 4*B*). The number of dead cells per infection site was analyzed (Fig. 4*C*). Compared to WT and *atrbohF*, significantly more dead cells were detected upon *Pst-avrRps4* inoculation in *atrbohD*. These results indicate that RBOHD negatively regulated cell death in plant-pathogen interactions.

The WT showed a restricted PCD, but an excessive

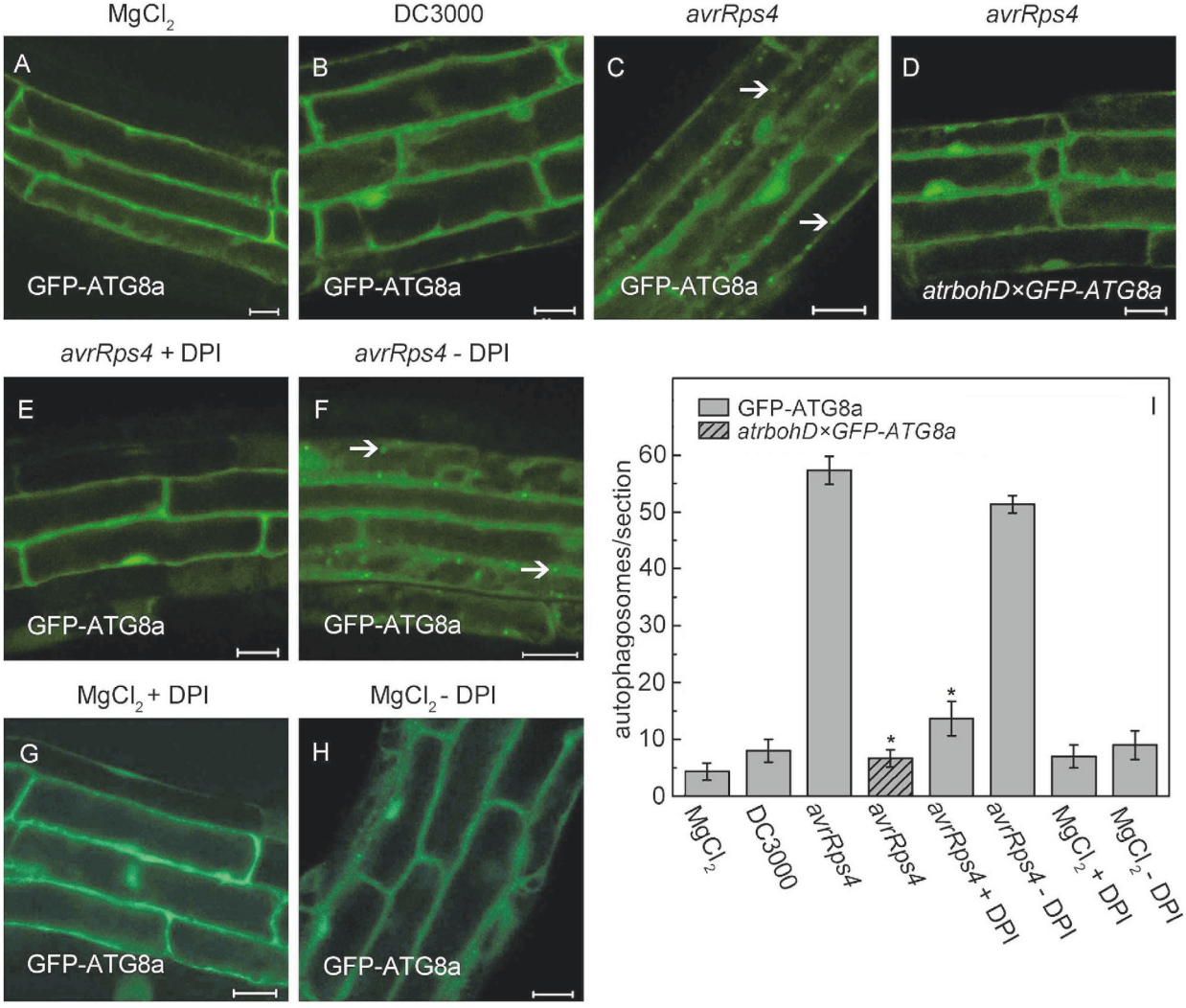

Fig. 2. Autophagy is regulated by the NADPH oxidase RBOHD pathway during avirulent pathogen infection. One-week-old GFP-ATG8a (*A* to *C; E* to *H*) and *atrbohD* × *GFP-ATG8a* (*D*) seedlings were inoculated with $MgCl_2$ or *Pst* DC3000 or *Pst-avrRps4* for 3 h (the *upper row*), or 1 h with additional 3 h mock ($MgCl_2$) or DPI treatments (the *middle and lower row*s). *Bars* = 20 μm. The number of autophagosome-related structures per root section was counted 3 h after inoculation (*I*). Mean and SE were calculated from three seedlings per treatment. Results were reproduced in three independent experiments. *Asterisks* indicate a significant difference from *atrbohD* × *GFP-ATG8a* treated by *avrRps4* ($P < 0.05$; Student's *t* test).

cell death was observed in *atrbohD* after infection with *Pst-avrRps4* (Fig. 3 and 4*B*). To determine if increased pathogen numbers caused the misregulation of cell death in the *atrbohD* mutant plants, we quantified the number of *Pst-avrRps4* cells in plant leaves. The number of *Pst-avrRps4* pathogens was not significantly different between *atrbohD* and WT at 2 or 4 dpi (Fig. 6), but cell death was unlimited in the *atrbohD* mutant indicating that uncontrolled cell death was not caused by a number of pathogens. The results suggest that RBOHD played a role

in limiting cell death, at least during the early phase of the plant defense response.

To analyze the function of autophagy genes during the immune response, plants were infected with *Pst-avrRps4,* and the transcription of autophagy genes were determined by semi-quantitative RT-PCR. To confirm that the expression of autophagy genes was caused by these conditions, SA-responsive pathogenesis resistant genes *PR1* and *PR2* as well as plant-pathogen interaction resistance gene *RPS4* were selected as pathogen defense markers (Hofius *et al*. 2009, Yoshimoto *et al*. 2009). Samples from the *Pst-avrRps4* inoculated WT and *atrbohD* mutant plants were collected at 0, 3, 6, 12, and 24 hpi. *ATG2*, *ATG7*, and *ATG8a* transcriptions were higher in WT than *atrbohD* after infection with *Pst-avrRps4* (Fig. 7). This suggests that autophagy might activate in WT, but not in the *atrbohD* mutant upon infection with avirulent pathogens. As expected, the transcription of *RPS4* increased in WT during *Pst-avrRps4* infection (Fig. 7). The transcription of *PR1* and *PR2* in the *atrbohD* mutant also increased, but the transcript accumulation of *PR1* in WT was clearly higher than in the *atrbohD* mutant. These results indicate that autophagy and disease resistance genes were activated by *avrRps4* in WT but not in the *atrbohD* mutants.

In conclusion, we present an example of the HR PCD

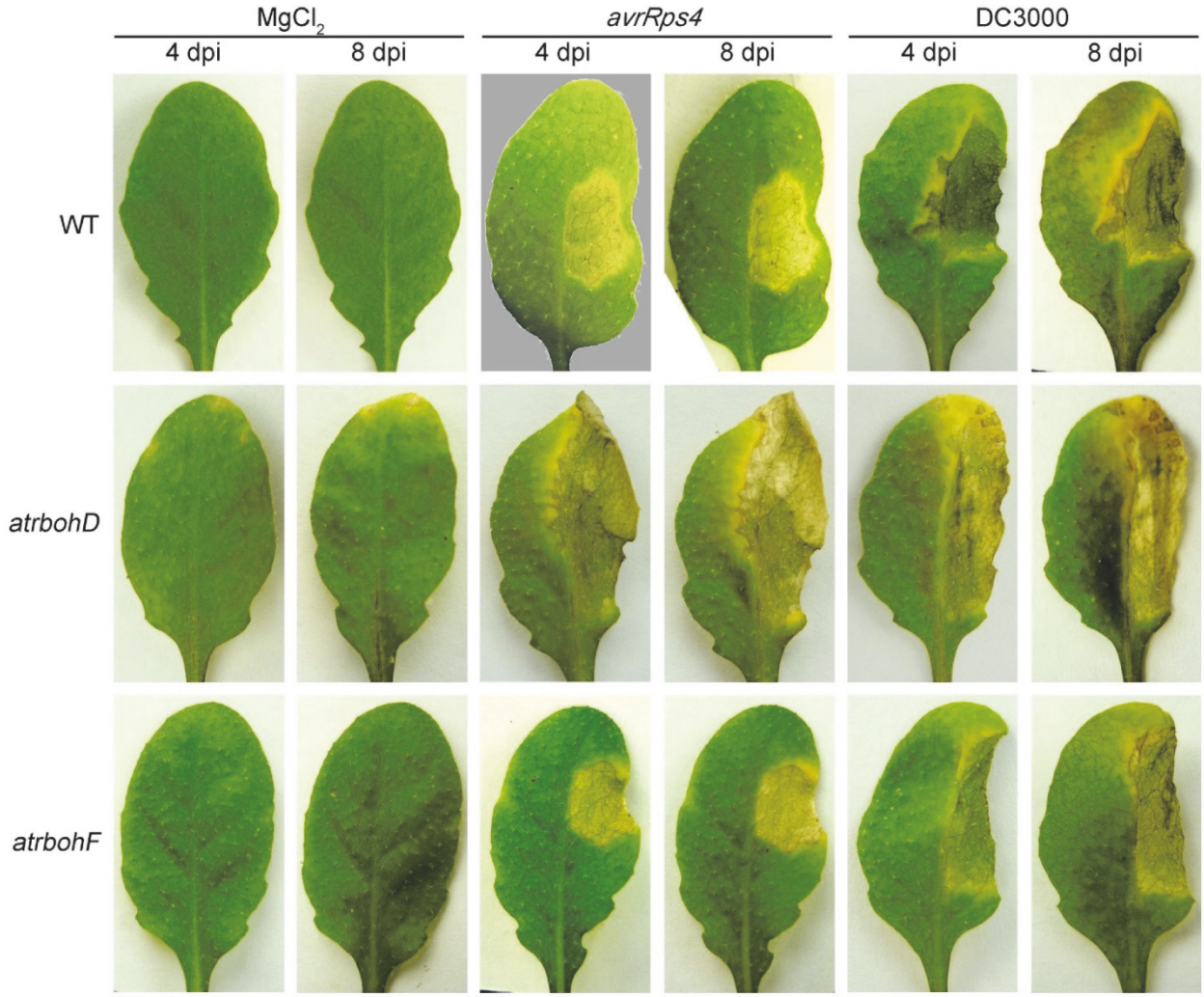

Fig. 3. RBOHD is required to limit the spread of *Pst-avrRps4*-induced cell death. WT, *atrbohD*, and *atrbohF* mutant plants were sprayed with $MgCl_2$ or infected with *Pst* DC3000 or *Pst-avrRps4*. Photographs were taken 4 or 8 dpi. These experiments were repeated three times with similar results.

pathway involving RBOHD and autophagy. The autophagy induction after avirulent pathogen infection in WT and the *atrbohF* mutant plants was accompanied by ROS burst and HR cell death. In contrast, autophagy could not be induced in the *atrbohD* mutants following infection with the avirulent pathogens, and excessive cell death occurred. These results suggest that avirulent pathogen-induced autophagy was activated by an RBOHD-dependent pathway, and that RBOHD contributed to autophagy and HR PCD.

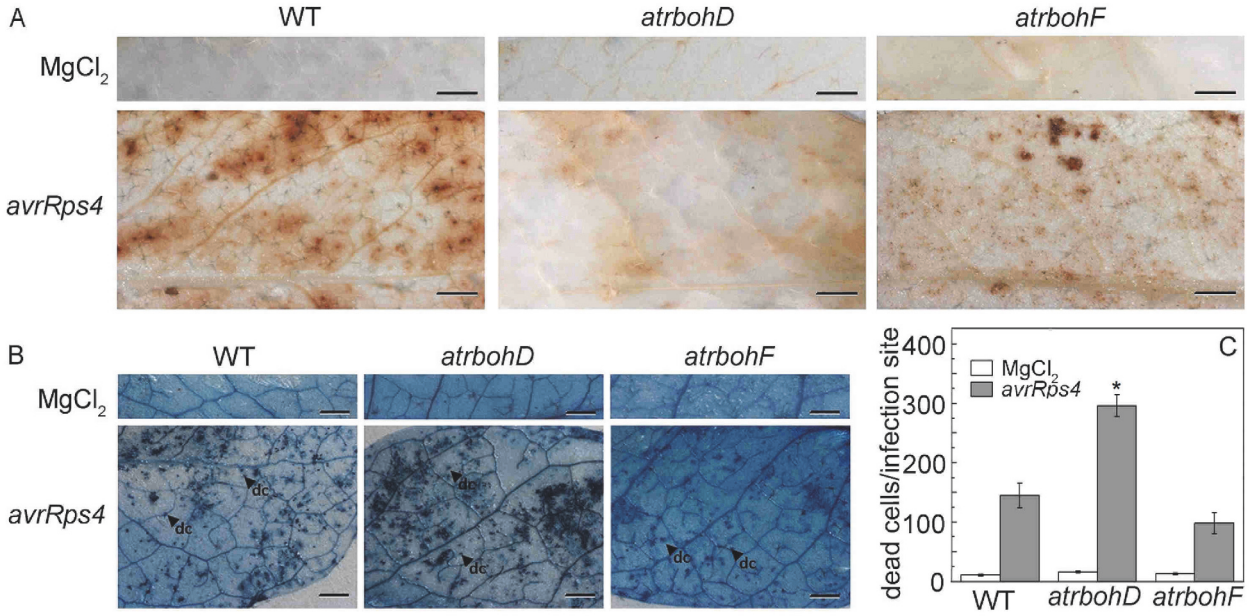

Fig. 4. *Pst-avrRps4*-induced ROS production (*A*) and cell death (*B*) in WT and *atrboh* mutants. WT, *atrbohD*, and *atrbohF* plants were infected with *Pst-avrRps4*. Photographs were taken 24 hpi. *Bars* = 200 µm. We acquired the similar results in three independent experiments. The number of dead cells (dc) per infection site was counted (*C*). Mean and SE were calculated from 10 independent areas of infection. *Asterisk* indicates a significant difference from WT treated with *avrRps4* ($P < 0.05$; Student's *t* test).

Discussion

Early production of ROS is the main signaling and defense response during pathogen invasion in plants (Levine *et al*. 1994, Hammond-Kosack and Jones 1996, Alvarez *et al*. 1998, Rose *et al*. 2006, Torres *et al*. 2006). We found that ROS were located at the cell membrane and accumulated 1 h after inoculation with *Pst-avrRps4*, and that their production was inhibited by DPI or in the *atrbohD* mutant (Fig. 5). In addition, ROS accumulation 24 hpi with *Pst-avrRps4* in the *atrbohD* mutant leaves was reduced when compared to WT and the *atrbohF* mutant (Fig. 4*A*). This suggests that ROS production acted as resistance defense response to *Pst-avrRps4* pathogen infection and was attributable to NADPH oxidase RBOHD in the plasma membrane.

What could be the physiological roles of RBOHD or ROS during plant immune response? The ROS can induce autophagy (Xiong *et al*. 2007) and further defense responses (Alvarez *et al*. 1998). Autophagy has been implicated as a protein degradation process induced under biotic or abiotic stresses including pathogen infection, nutrient starvation, and unfavorable growth conditions (Liu *et al*. 2005, 2009, Slavíková *et al*. 2005). Autophagy also occurs constitutively in roots of plants (Liu *et al*. 2009, 2010). Autophagy can be induced by SA analog benzothiadiazole (BTH) as well as by avirulent strains of *Pst* DC3000 that harbor avirulence genes *avrRpm1* or *avrRps4* (Fig. 2 Suppl.) The infection of a plant can lead to an immune response in the root as part of systemic acquired resistance, and similar immune response mechanisms have been identified in various plant species (Van Loon *et al.* 1998, Iavicoli *et al*. 2003, Millet *et al*. 2010). Therefore, the role played by the root in protecting the plant against pathogen invasion makes it an appropriate target for the study of plant-pathogen innate immunity. We demonstrated the induction of autophagy in the WT plants after infection with *Pst-avrRps4* (Fig. 1), and we further monitored autophagy by using GFP-ATG8a (Fig. 2). The induction of autophagy by *Pst-avrRps4* was consistent with previous findings that GFP-ATG8a is transiently expressed in the WT plants infected with avirulent pathogens but not virulent *Pst* DC3000 (Hofius *et al*. 2009). Further, we found that autophagy was blocked by DPI after inoculation with *Pst-avrRps4* in the GFP-ATG8a seedlings (Fig. 2). The *atrbohD* mutant and *atrbohD* × *GFP-ATG8a* seedlings also did not show any autophagosomes, whereas the GFP-ATG8a, WT, and *atrbohF* mutant background accumulated auto-phagosomes abundantly after infection with *Pst-avrRps4* (Figs. 1 and 2). These results coincide with the upregulation of autophagy-related genes *ATG2*, *ATG7*, and *ATG8a* in WT (Figs. 1 and 7). The *AtrbohD* knock-out mutation reduced ROS accumulation and blocked the autophagy pathway (Figs. 1 and 4*A*). These results indicate that both RBOHD and ROS are potential signaling molecules that mediate autophagy. This is consistent with the results of studies demonstrating that autophagy can be induced by avirulent pathogens (Hofius *et al*. 2009) or H_2O_2 (Xiong *et al*. 2007).

During plant-pathogen interactions, autophagy is required to restrict HR PCD initiated during the innate immune response caused by avirulent pathogens (Patel and Dinesh-Kumar 2008). The most striking characteristics of HR are rapid cell death at the infection site and the activation of a series of defense responses (McDowell and Dangl 2000). For instance, studies have shown that HR PCD is the most important and obvious response to pathogen invasions because it limits pathogens at the infection site by killing cells in the susceptible regions in order to protect the plant (Liu *et al*. 2005, Seay *et al*. 2009). Autophagy-deficient mutant plants fail to limit the spread of cell death and lose the ability to resist infection (Patel and Dinesh-Kumar 2008, Yoshimoto *et al*. 2009). The *AtrbohD* mutants showed an enhanced cell death compared to WT and *atrbohF* after being infected with *Pst-avrRps4* (Figs. 3 and 4). Moreover, the number of *Pst-avrRps4* pathogens was not significantly different in the *atrbohD* mutant plant compared to WT at 2 and 4 dpi (Fig. 6*B*) thus indicating that the cell death phenotype was not due to the growth of pathogens. We also found that the *atrbohD* mutants exhibited the spread of the *Pst-avrRps4*-induced cell death phenotype in the case of older rather than younger plants (Fig. 3), and this apparent discrepancy was likely due to dependency of SA content on the plant age. It was shown that SA content increases and the spread of cell death progresses after infection with *A. brassicicola* strain CBS 125088 in an

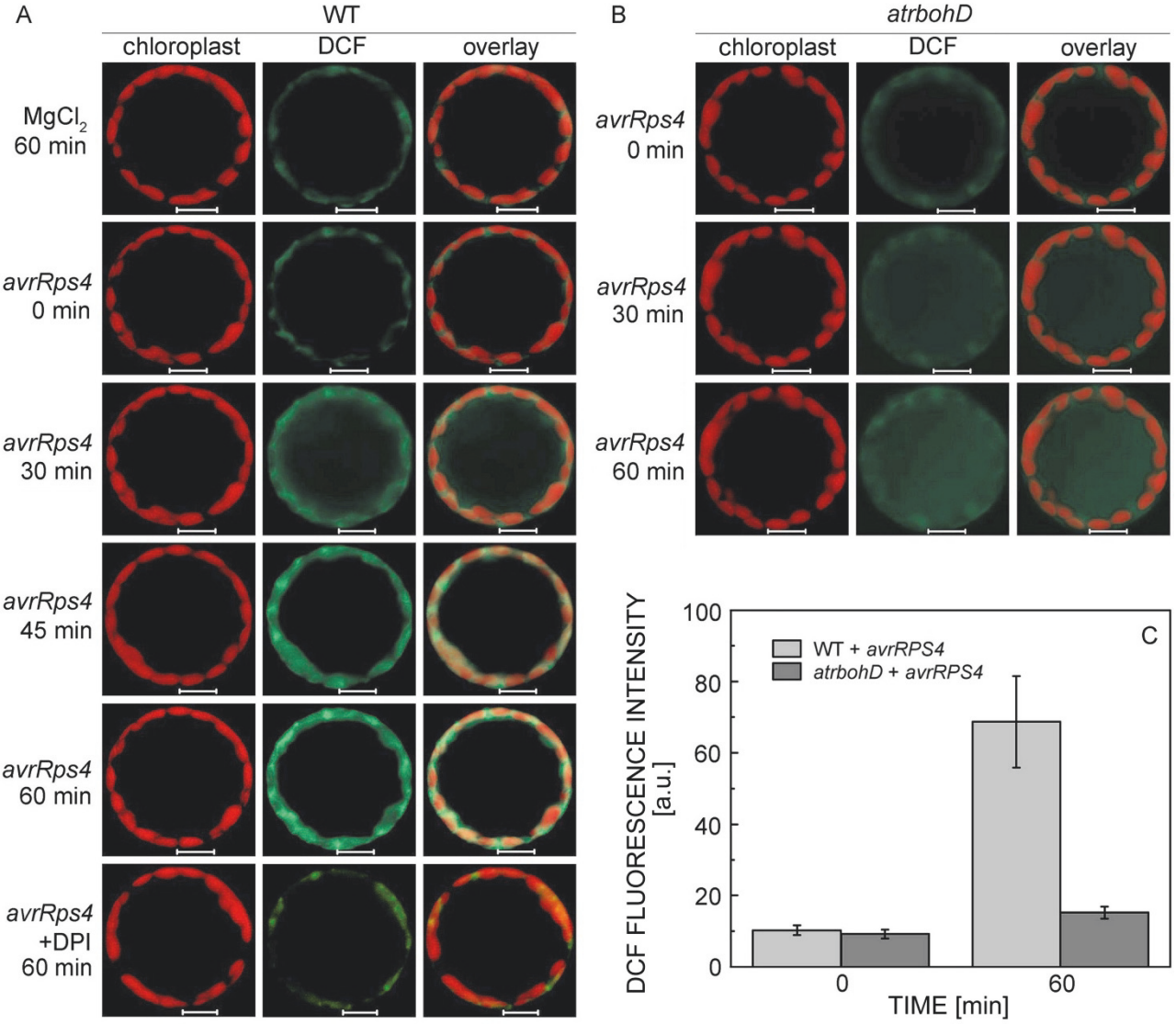

Fig. 5. Localization and accumulation of *Pst-avrRps4*-induced ROS. The protoplasts of 6-week-old WT (*A*) or *atrbohD* (*B*) mutant leaves were inoculated with *Pst-avrRps4* for 30 min and subsequently stained with DCF and observed during the time course of 60 min. *Bars* = 10 μm. The DCF fluorescence intensity (*C*). Means ± SE of three independent replicates.

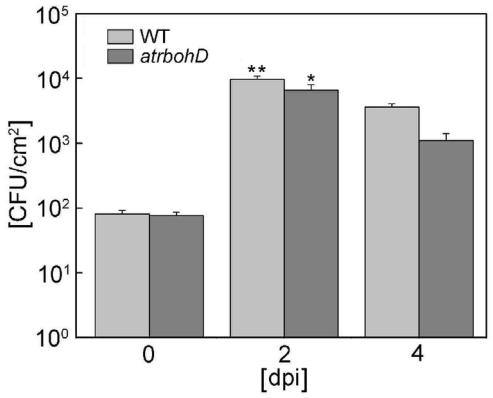

Fig. 6. Growth of avirulent *Pst-avrRps4* in WT or *atrbohD*. Bacterial growth quantification of *Pst-avrRps4* on WT and *atrbohD* at 0, 2, and 4 dpi. *Error bars* represent the standard deviation of three samples per experiment; the experiment is representative of three independent replicates. Significant differences from WT treated by *avrRps4* at * - $P < 0.05$; ** - $P < 0.01$.

atrbohD mutant (Pogány *et al*. 2009). The SA analog BTH accelerates pathogen-induced cell death in both WT and *atrbohD* plants, but the *atrbohD* plants exhibit an increased spread of cell death compared to WT (Pogány *et al*. 2009). This is similar to what Yoshimoto *et al.* (2009) observed in the spread of cell death phenotypes of autophagy-deficient mutants leaves of older plants. The phenotype age dependency is likely due to increased levels of SA in older autophagy-deficient mutants as well as the role of SA in cell death (Yoshimoto *et al*. 2009). These results suggest that cell death was caused by SA, and that the hyperaccumulation of SA was caused by autophagy-deficiency. Similar phenotypes of *atrbohD* and autophagy-deficient mutants when infected with avirulent pathogens are due to an autophagy defect. This would mean that autophagy is activated by an NADPH oxidase RBOHD-dependent pathway during avirulent pathogen infection.

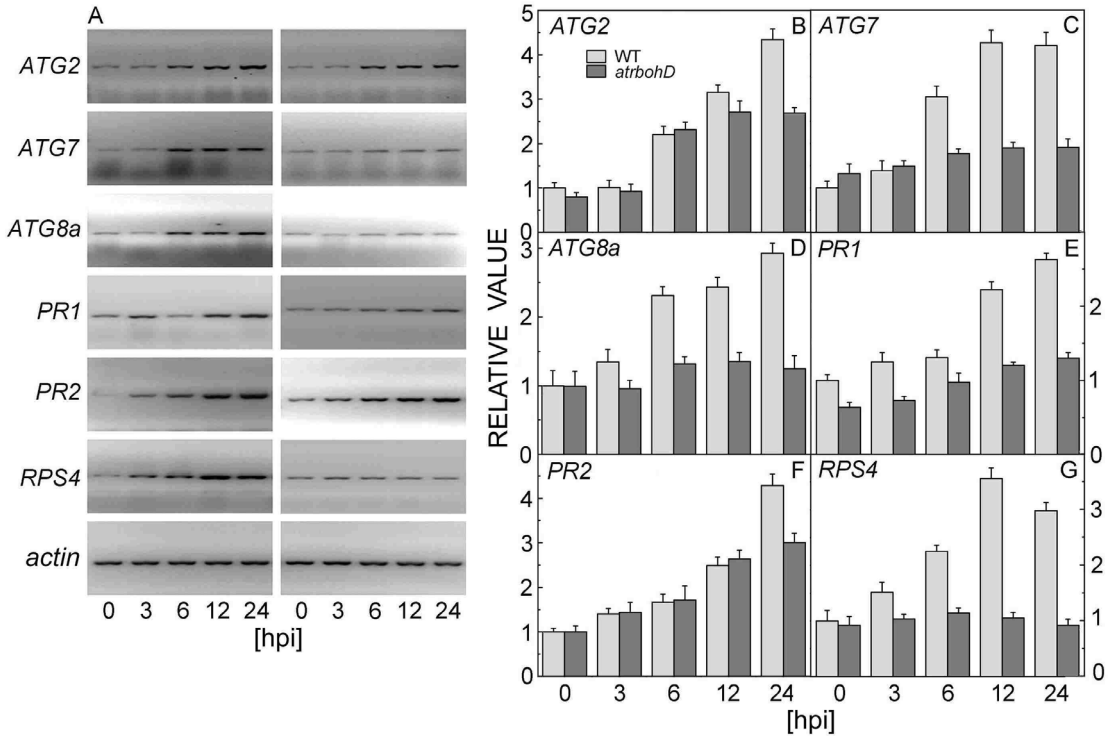

Fig. 7. Expression patterns of autophagy and pathogen-related genes in WT and *atrbohD* mutant plants. WT and *atrbohD* mutant leaves were inoculated with *Pst-avrRps4*. Total RNA was extracted from leaves which were collected at indicated time points and detection by RT-PCR followed. *ACTIN* was used as internal control. *B* to *G* - the values on the y-axis are relative fluorescence intensities; control intensity was set as 1. Means and SE were calculated from three independent experiments.

In conclusion, our results suggest that RBOHD-dependent production of ROS plays an ambiguous role in a pathogen-induced autophagy and HR cell death (Fig. 8). On one hand, RBOHD-derived ROS can serve as secondary messengers to activate autophagy. However, ROS can trigger not only cell death due to damage after infection, but they also inhibit the spread of cell death to neighbouring cells. The results obtained in this study provide a further insight into the regulatory mechanisms of pathogen-triggered RBOHD-dependent autophagy and HR cell death.

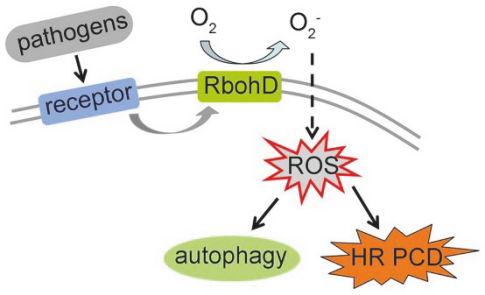

Fig. 8. A model proposed for the RBOHD function in pathogen-induced autophagy and PCD. During pathogen infection, ROS are accumulated by functional RBOHD. As signal, ROS triggers autophagy and PCD.

References

Alvarez, M.E., Pennell, R.I., Meijer, P.J., Ishikawa, A., Dixon, R.A., Lamb, C.: Reactive oxygen intermediates mediate a systemic signal network in the establishment of plant immunity. - Cell **92**: 773-784, 1998.

Bi, Y., Chen, W., Zhang, W., Zhou, Q., Yun, L., Xing, D.: Production of reactive oxygen species, impairment of photosynthetic function and dynamic changes in mitochondria are early events in cadmium induced cell death in *Arabidopsis thaliana*. - Biol. Cell **101**: 629-643, 2009.

Bolwell, G.P., Davies, D.R., Gerrish, C., Auh, C.K., Murphy, T.M.: Comparative biochemistry of the oxidative burst produced by rose and French bean cells reveals two distinct mechanisms. - Plant Physiol. **116**: 1379-1385, 1998.

Doelling, J.H., Walker, J.M., Friedman, E.M., Thompson, A.R., Vierstra, R.D.: The APG8/12-activating enzyme APG7 is required for proper nutrient recycling and senescence in *Arabidopsis thaliana*. - J. biol. Chem. **277**: 33105-33114, 2002.

Gao, X., Chen, X., Lin, W., Chen, S., Lu, D., Niu, Y., Li, L., Cheng, C., McCormack, M., Sheen, J., Shan, L., He, P.: Bifurcation of *Arabidopsis* NLR immune signaling via Ca^{2+}-dependent protein kinases. - PLoS Patholog. **9**: e1003127, 2013.

Hammond-Kosack, K.E., Jones, J.D.: Resistance gene-dependent plant defense responses. - Plant Cell **8**: 1773-1791, 1996.

Hanaoka, H., Noda, T., Shirano, Y., Kato, T., Hayashi, H., Shibata, D., Tabata, S., Ohsumi, Y.: Leaf senescence and starvation-induced chlorosis are accelerated by the disruption of an *Arabidopsis* autophagy gene. - Plant Physiol. **129**: 1181-1193, 2002.

Hofius, D., Schultz-Larsen, T., Joensen, J., Tsitsigiannis, D.I., Petersen, N.H., Mattsson, O., Jorgensen, L.B., Jones, J.D., Mundy, J., Petersen, M.: Autophagic components contribute to hypersensitive cell death in *Arabidopsis*. - Cell **137**: 773-783, 2009.

Iavicoli, A., Boutet, E., Buchala, A., Métraux, J.P.: Induced systemic resistance in *Arabidopsis thaliana* in response to root inoculation with *Pseudomonas fluorescens* CHA0. - MPMI **16**: 851-858, 2003.

Inoue, Y., Suzuki, T., Hattori, M., Yoshimoto, K., Ohsumi, Y., Moriyasu, Y.: AtATG genes, homologs of yeast autophagy genes, are involved in constitutive autophagy in *Arabidopsis* root tip cells. - Plant Cell Physiol. **47**: 1641-1652, 2006.

Jiang, M., Zhang, J.: Involvement of plasma-membrane NADPH oxidase in abscisic acid- and water stress-induced antioxidant defense in leaves of maize seedlings. - Planta **215**: 1022-1030, 2002.

Lai, Z., Wang, F., Zheng, Z., Fan, B., Chen, Z.: A critical role of autophagy in plant resistance to necrotrophic fungal pathogens. - Plant J. **66**: 953-968, 2011.

Lam, E.: Controlled cell death, plant survival and development. - J. mol. cell. Biol. **5**: 305-315, 2004.

Levine, A., Tenhaken, R., Dixon, R., Lamb, C.: H_2O_2 from the oxidative burst orchestrates the plant hypersensitive disease resistance response. - Cell **79**: 583-593, 1994.

Liu, J., Zhou, J., Xing, D.: Phosphatidylinositol 3-kinase plays a vital role in regulation of rice seed vigor via altering NADPH oxidase activity. - PLoS One **7**: e33817, 2012.

Liu, Y., Bassham D.C.: TOR is a negative regulator of autophagy in *Arabidopsis thaliana*. - PLoS One **5**: e11883, 2010.

Liu, Y., Schiff, M., Czymmek, K., Tallóczy, Z., Levine, B., Dinesh-Kumar, S.P.: Autophagy regulates programmed cell death during the plant innate immune response. - Cell **121**: 567-577, 2005.

Liu, Y., Xiong, Y., Bassham, D.C.: Autophagy is required for tolerance of drought and salt stress in plants. - Autophagy **5**: 954-963, 2009.

Mackey, D., Belkhadir, Y., Alonso, J.M., Ecker, J.R., Dangl, J.L.: *Arabidopsis* RIN4 is a target of the type III virulence effector AvrRpt2 and modulates RPS2-mediated resistance. - Cell **112**: 379-389, 2003.

McDowell, J.M., Dangl, J.L.: Signal transduction in the plant immune response. - Trends Biochem. Sci. **25**: 79-82, 2000.

Millet, Y.A., Danna, C.H., Clay, N.K., Songnuan, W., Simon, M.D., Werck-Reichhart, D., Ausubel, F.M.: Innate immune responses activated in *Arabidopsis* roots by microbe-associated molecular patterns. - Plant Cell **22**: 973-990, 2010.

Ogasawara, Y., Kaya, H., Hiraoka, G., Yumoto, F., Kimura, S., Kadota, Y., Hishinuma, H., Senzaki, E., Yamagoe, S., Nagata, K., Nara, M., Suzuki, K., Tanokura, M., Kuchitsu, K.: Synergistic activation of the *Arabidopsis* NADPH oxidase AtrbohD by Ca^{2+} and phosphorylation. - J. biol. Chem. **283**: 8885-8892, 2008.

Patel, S., Dinesh-Kumar, S.P.: *Arabidopsis* ATG6 is required to limit the pathogen-associated cell death response. - Autophagy **4**: 20-27, 2008.

Pogány, M., Von Rad, U., Grün, S., Dongó, A., Pintye, A., Simoneau, P., Bahnweg, G., Kiss, L., Barna, B., Durner, J.: Dual roles of reactive oxygen species and NADPH oxidase RBOHD in an *Arabidopsis-Alternaria* pathosystem. - Plant Physiol. **151**: 1459-1475, 2009.

Rose, T.L., Bonneau, L., Der, C., Marty-Mazars, D., Marty, F.: Starvation-induced expression of autophagy-related genes in *Arabidopsis*. - Biol. Cell **98**: 53-67, 2006.

Scherz-Shouval, R., Shvets, E., Fass, E., Shorer, H., Gil, L., Elazar, Z.: Reactive oxygen species are essential for autophagy and specifically regulate the activity of Atg4. - EMBO J. **26**: 1749-1760, 2007.

Seay, M., Hayward, A.P., Tsao, J., Dinesh-Kumar, S.P.: Something old, something new: plant innate immunity and autophagy. - Curr. Topics Microbiol. **335**: 287-306, 2009.

Seay, M., Patel, S., Dinesh-Kumar, S.P.: Autophagy and plant innate immunity. - Cell Microbiol. **8**: 899-906, 2006.

Slavíková, S., Shy, G., Yao, Y., Glozman, R., Levanony, H., Pietrokovski, S., Elazar, Z., Galili, G.: The autophagy-associated *Atg8* gene family operates both under favourable growth conditions and under starvation stresses in *Arabidopsis* plants. - J. exp. Bot. **56**: 2839-2849, 2005.

Thompson, A.R., Doelling, J.H., Suttangkakul, A., Vierstra, R.D.: Autophagic nutrient recycling in *Arabidopsis* directed by the ATG8 and ATG12 conjugation pathways. - Plant Physiol. **138**: 2097-2110, 2005.

Torres, M.A., Dangl, J.L.: Functions of the respiratory burst oxidase in biotic interactions, abiotic stress and development. - Curr. Opin. Plant Biol. **8**: 397-403, 2005.

Torres, M.A., Dangl, J.L., Jones, J.D.: *Arabidopsis* gp91^{phox} homologues AtrbohD and AtrbohF are required for accumulation of reactive oxygen intermediates in the plant defense response. - Proc. nat. Acad. Sci. USA **99**: 517-522, 2002.

Torres, M.A., Jones, J.D., Dangl, J.L.: Reactive oxygen species signaling in response to pathogens. - Plant Physiol. **141**: 373-378, 2006.

Van Loon, L.C., Bakker, P., Pieterse, C.M.J.: Systemic resistance induced by rhizosphere bacteria. - Annu. Rev. Phytopathol. **36**: 453-483, 1998.

Wang, Y., Nishimura, M.T., Zhao, T., Tang, D.: ATG2, an autophagy-related protein, negatively affects powdery mildew resistance and mildew-induced cell death in *Arabidopsis*. - Plant J. **68**: 74-87, 2011.

Wojtaszek, P.: Oxidative burst: an early plant response to pathogen infection. - Biochem. J. **322**: 681-692, 1997.

Xiong, Y., Contento, A.L., Bassham, D.C.: AtATG18a is required for the formation of autophagosomes during nutrient stress and senescence in *Arabidopsis thaliana*. - Plant J. **42**: 535-546, 2005.

Xiong, Y., Contento, A.L., Nguyen, P.Q., Bassham, D.C.: Degradation of oxidized proteins by autophagy during oxidative stress in *Arabidopsis*. - Plant Physiol. **143**: 291-299, 2007.

Yoshimoto, K., Jikumaru, Y., Kamiya, Y., Kusano, M., Consonni, C., Panstruga, R., Ohsumi, Y., Shirasu, K.: autophagy negatively regulates cell death by controlling NPR1-dependent salicylic acid signaling during senescence and the innate immune response in *Arabidopsis*. - Plant Cell **21**: 2914-2927, 2009.

Yun, L.J., Chen, W.L.: SA and ROS are involved in methyl salicylate-induced programmed cell death in *Arabidopsis thaliana.* - Plant Cell Rep. **30**: 1231-1239, 2011.